Title

No circadian clock-gene circuit in the generation of cellular bioluminescence rhythm of *CaMV35S::PtRLUC* in duckweed

Author List

Emiri Watanabe[1,2], Tomoaki Muranaka[1,3], Shunji Nakamura[1,4], Minako Isoda[1], Shogo Ito[1], Tokitaka Oyama[1,*]

*Corresponding author (email): oyama.tokitaka.8w@kyoto-u.ac.jp

Author Affiliation

1. Department of Botany, Graduate School of Science, Kyoto University, Kitashirakawa-Oiwake-cho, Sakyo-ku, Kyoto, 606-8502, Japan

Present addresses

2. Department of Complexity Science and Engineering, Graduate School of Frontier Sciences, The University of Tokyo, Kashiwa, Chiba 277-8561, Japan
3. Faculty of Agriculture, Kagoshima University, Korimoto 21-24-1, Kagoshima, 890-0065, Japan
4. Department of Biological Sciences, Graduate School of Science, The University of Tokyo, Tokyo, 113- 0033, Japan

Summary

The circadian clock is responsible for the temporal regulation of various physiological phenomena in plants. Individual cells contain the cellular circadian clock consisting of the clock gene circuit. Physiological rhythms are coordinated in the plant body in an orderly manner. Multiple circadian rhythms with different free-running periods (FRPs) can coexist in the same plant. In addition to different circadian properties between tissues/organs, uncoupled circadian rhythms in the same cell have been reported. The relationship between the cellular circadian clock and the various circadian outputs with different FRPs is currently unknown. Using a dual-color bioluminescence monitoring system in *Lemna minor* transfected with the *AtCCA1::LUC+* and *CaMV35S::PtRLUC* reporters, cellular bioluminescence rhythms with different FRPs were detected in the same cells. Co-transfection experiments with the two reporters and a clock gene overexpressing effector revealed that the circadian properties of the *AtCCA1::LUC+* rhythm, but not those of the *CaMV35S::PtRLUC* rhythm, were altered in the cells with a dysfunctional clock gene circuit. This indicates that the *AtCCA1::LUC+* rhythm is a direct output of the cellular circadian clock while the *CaMV35S::PtRLUC* rhythm is not. After plasmolysis, the *CaMV35S::PtRLUC* rhythm disappeared while the *AtCCA1::LUC+* rhythm persisted. This suggested that *CaMV35S::PtRLUC* is a symplast/apoplast mediated circadian rhythm generated at an organismal level. This idea is consistent with the observation that the phases of *CaMV35S::PtRLUC* cellular rhythms remain highly synchronized while those of *AtCCA1::LUC+* rhythms gradually get desynchronized. The plant circadian system consists of both cell-autonomous rhythms and non-cell-autonomous rhythms that are unaffected by the cellular clock.

Keywords

circadian rhythms, clock genes, dual-color bioluminescence, *Lemna minor*, luciferases, non-cell-autonomous rhythm, single-cell monitoring

Introduction

Many physiological phenomena in plants show circadian rhythms.[1] The circadian clock is a cell-autonomous system composed of a number of clock genes that form transcription–translation feedback loops (TTFLs).[2,3] In *Arabidopsis*, dawn-expressed *CIRCADIAN CLOCK-ASSOCIATED 1* (*CCA1*), *LATE ELONGATED HYPOCOTYL* (*LHY*), morning-to-evening-expressed *PSEUDO-RESPONSE REGULATOR* (*PRR*) family, evening-to-night-expressed *EARLY FLOWERING 3* (*ELF3*) , *ELF4*, and *LUX ARRHYTHMO* (*LUX*) repress genes expressed during earlier phases. The F-box protein ZEITLUPE (ZTL) affects the TTFLs by temporal promotion of proteasomal degradation of PRR members. Disruption and/or overexpression of these clock genes impairs the circadian rhythm.[2,3] The TTFL oscillator governs the circadian rhythms of various physiological processes in plants, and mutations in clock genes alter these circadian rhythms.[4,5]

Physiological rhythms with different free-running periods (FRPs) have been observed in plants.[6] For example, rhythms in cytosolic free calcium (Ca^{2+}) levels have a different FRP from that of *Lhcb* gene expression in tobacco.[7] Differences in the FRPs of bioluminescence rhythms were observed in *Arabidopsis* seedlings expressing a firefly luciferase under circadian promoters *CHALCONE SYNTHASE* (*CHS*), *CHLOROPHYLL A/B BINDING PROTEIN* (*CAB*), *PHYTOCHROME B* (*PHYB*) and *CATALASE 3* (*CAT3*).[8–10] Tissue-specific modulation of the TTFL is considered to be a contributing factor to these different FRPs.[6,11] These distinct oscillators can bring about uncoupled rhythms between tissues/organs and influence the coordination of physiological processes at the organismal level.

In addition to tissue/organ-specific circadian rhythms, intracellular uncoupling of two circadian rhythms has also been reported in plant cells.[12] Bioluminescence of a luciferase driven by a constitutive promoter showed a circadian rhythm in various duckweeds, and *CaMV35S::PtRLUC* (a modified click beetle red color luciferase gene) showed bioluminescence rhythms uncoupled from those of *AtCCA1::LUC+* (a firefly yellow-green luciferase gene) in individual cells in *Lemna minor*.[12,13] The uncoupled rhythms were detected using a dual-color bioluminescence monitoring system at a single-cell level, in which *AtCCA1::LUC+* and *CaMV35S::PtRLUC* reporters were simultaneously transfected into the cells in the duckweed plant by particle bombardment. The intracellular uncoupling was observed as inconsistent phase relation and different FRPs under prolonged and constant light conditions. The *AtCCA1::LUC+* bioluminescence rhythm was shown to be cell-autonomously generated under the control of the TTFL in individual cells, through functional analysis by co-transfecting an effector (overexpression, knockdown and knockout of clock genes) with the circadian reporter.[14–16] In duckweed plants, desynchronization of the cell-autonomous circadian clock occurs between cells in the same tissue under constant conditions, although weak cell-to-cell interaction influencing their phases is expected.[17,18] However, it is unclear how the intracellular uncoupling between *AtCCA1::LUC+* and *CaMV35S::PtRLUC* bioluminescence rhythms happens in individual cells, as the mechanism underlying the *CaMV35S::PtRLUC* bioluminescence rhythm is currently unknown.[12] Cell autonomy and the direct involvement of TTFL are questionable. In this study, we

85 performed co-transfection using circadian reporters and clock gene overexpressing effectors in a
86 dual-color bioluminescence monitoring system at a single-cell level. We also analyzed the effects of
87 plasmolysis on the cellular circadian rhythms. We show that the *CaMV35S::PtRLUC* bioluminescence
88 rhythm is non-cell-autonomously generated, without direct regulation by the clock-gene circuit.
89
90
91 **Results**
92 Differences in the free-running periods and the intercellular synchrony between *AtCCA1::LUC*+ and
93 *CaMV35S::PtRLUC* bioluminescence rhythms
94 In order to directly compare circadian properties of the bioluminescence rhythms between the two
95 reporters, we performed dual-color bioluminescence monitoring at a single-cell level.[12] Circadian
96 reporters with different luminescence colors, *AtCCA1::LUC*+ (yellow-green) and *CaMV35S::PtRLUC*
97 (red), were introduced into *L. minor* cells (epidermal and mesophyll cells) through particle
98 bombardment (Figure 1A). The bioluminescence of individual cells was observed using an EM-CCD
99 camera with a filter exchanger containing green-pass and red-pass filters, and the cellular
100 luminescence intensities of each reporter were reconstructed based on a set of filtered luminescence
101 images (Figure 1B). A set of luminescence images was acquired every hour according to the time
102 schedule shown in Figure 1C.
103 *AtCCA1::LUC*+ and *CaMV35S::PtRLUC* bioluminescence rhythms of 37 cells from the same
104 frond under constant light are shown in Figure 2. As shown in Figure 2A and 2B, most cells showed
105 circadian rhythms of both bioluminescence reporters. The FRP and relative amplitude error (RAE) of
106 each luminescence trace were calculated using the fast Fourier transform non-linear least squares
107 (FFT-NLLS) method.[19] The RAE value represents the degree of confidence of rhythmicity, ranging
108 from 0 (complete sine-fitting) to 1 (arrhythmic). In this study, bioluminescence traces with RAE < 0.2
109 were defined as rhythmic, and the rest were defined as arrhythmic. Every cell showed
110 *CaMV35S::PtRLUC* rhythm, while 33 cells (89%) showed *AtCCA1::LUC*+ rhythm (Table S1).
111 Although the bioluminescence traces of *CaMV35S::PtRLUC* in all cells were judged to be rhythmic,
112 the *CaMV35S::PtRLUC* rhythm looked lower in amplitude than the *AtCCA1::LUC*+ rhythm (Figure 2A
113 and 2B). FRPs of *AtCCA1::LUC*+ and *CaMV35S::PtRLUC* rhythms were distributed differently, with
114 values of 25.5 ± 0.8 h and 24.7 ± 0.6 h, respectively (Figure 2C and Table S1). The FRP of the
115 *CaMV35S::PtRLUC* rhythm was significantly shorter than that of the *AtCCA1::LUC*+ rhythm in the
116 same set of cells in a frond (Welch *t*-test, $p=3.8\times10^{-13}$). The shorter FRP of *CaMV35S::PtRLUC* rhythm
117 was also observed in *L. minor* plants that had grown under constant light without experiencing an
118 entrainment dark stimulus.[12]
119 Figures 2D and 2E show the phase distributions and degrees of synchrony (synchronization
120 index: SI) at t=24 h and 96 h for *AtCCA1::LUC*+ rhythms and *CaMV35S::PtRLUC* rhythms,
121 respectively. The SI of *AtCCA1::LUC*+ rhythm was 0.96 at t=24 h and decreased to 0.66 at t=96 h.
122 The SI of *CaMV35S::PtRLUC* at t=24 h was 0.85, which was almost the same as that at t=96 h (0.79).

123 The SI of *AtCCA1::LUC+* rhythm continuously decreased during the constant light condition, while
124 that of *CaMV35S::PtRLUC* rhythm was stable (Figure 2F). Previous studies found that
125 desynchronization of *AtCCA1::LUC+* cellular rhythms occurred under constant light condition in
126 duckweed plants that had been entrained.[17,18] The higher synchrony of *CaMV35S::PtRLUC* cellular
127 rhythms in fronds with asynchronous *AtCCA1::LUC+* cellular rhythms has also been reported in plants
128 that had not experienced entrainment.[12]

129 In *L. minor* transgenic plants carrying an *AtCCA1::LUC+* reporter, the circadian behaviors of
130 bioluminescence showed a variation among fronds.[18] To investigate variations in cellular circadian
131 behaviors of *AtCCA1::LUC+* and *CaMV35S::PtRLUC* rhythms among fronds, we studied four fronds
132 (including that shown in Figure 2) through dual-color bioluminescence monitoring (dual#1-#4; Table
133 S1) and three fronds for each of the reporters through single reporter bioluminescence monitoring
134 (sCCA1#1-#3, s35S#1-#3; Table S2). The mean FRPs of *AtCCA1::LUC+* rhythm determined by dual-
135 color monitoring were 25.3-27.4 h, and those of *CaMV35S::PtRLUC* rhythm were 24.0-25.0 h (Figure
136 3A). In three out of the four fronds, the FRPs of *CaMV35S::PtRLUC* rhythm were significantly shorter
137 than those of *AtCCA1::LUC+* rhythm. This was also confirmed by comparing FRPs of the two rhythms
138 in individual cells; 97 out of 116 cells showed shorter FRPs in case of *CaMV35S::PtRLUC* rhythm
139 (Figure 3B). Interestingly, the *CaMV35S::PtRLUC* rhythm (s^2 = 0.67) showed lower FRP variation
140 between cells than the *AtCCA1::LUC+* rhythm (s^2 = 2.60) (*F* test, $p = 3.2\times10^{-12}$). The FRP variation is
141 linked to desynchronization of cellular rhythms in a frond.[17] In fact, the SI of *AtCCA1::LUC+* rhythm in
142 each frond continuously decreased while that of *CaMV35S::PtRLUC* was stable (Figure 2F and S1A).
143 These differences in cellular circadian properties between the *AtCCA1::LUC+* and
144 *CaMV35S::PtRLUC* rhythms were confirmed through single reporter bioluminescence monitoring
145 (Table S2, Figure S1BC). With respect to the phase relation, the mean peak phases of the
146 bioluminescence rhythms showed higher variation between fronds in dual-reporter experiments
147 (*AtCCA1::LUC+*, 4.307-5.204 rad; *CaMV35S::PtRLUC*, 0.334-1.890 rad) than those in single reporter
148 experiments (*AtCCA1::LUC+*, 5.284-5.654 rad; *CaMV35S::PtRLUC*, 0.706-1.087 rad) (Tables S1 and
149 S2). The higher phase variation in the dual-reporter experiments might be due to noise amplification
150 in the process of reconstruction for luminescence intensities of both reporters.

151 In summary, we noted the shorter period and higher synchrony of the *CaMV35S::PtRLUC*
152 rhythm than the *AtCCA1::LUC+* rhythm in the same frond through dual-color bioluminescence
153 monitoring at a single cell level. The differences in the FRPs and the intercellular synchrony between
154 the two bioluminescence rhythms indicate differences in the mechanisms of oscillation generation
155 between them.

156

157 <u>Robustness of *CaMV35S::PtRLUC* bioluminescence rhythm against clock gene overexpression at</u>
158 <u>the single cell level</u>

159 We co-transfected the overexpressing effector of each of the three *L. minor* clock gene homologs,
160 *LmZTL*, *LmLUX*, and *LmELF3*, with the dual reporters to examine their effects on the *AtCCA1::LUC+*

161 and *CaMV35S::PtRLUC* bioluminescence rhythms in the same cell (Table S1 and Figure S2). In
162 *Arabidopsis*, it was reported that moderate and strong overexpression of *ZTL* caused shortening of
163 FRP and loss of circadian rhythms, respectively.[20] In *L. minor*, *LmZTL* overexpression caused a
164 destabilization of *AtCCA1::LUC*+ rhythm (Table S1). When RAE<0.2 was used as a criterion for
165 rhythmic cells, only 21% of the analyzed cells showed circadian rhythms in the experiment dual-
166 ZTLox#1 (Figure 4A and 4C). Without the *CaMV35S::LmZTL* effector, most cells showed
167 *AtCCA1::LUC*+ rhythm (Figure 2C and Table S1). This indicated that overexpression of *LmZTL*
168 disrupted the clock gene circuit in the transfected cells. By contrast, overexpression of *LmZTL* did not
169 affect the *CaMV35S::PtRLUC* rhythm in the analyzed cells. Every cell showed a waveform rhythm
170 similar to that observed in experiments without the *CaMV35S::LmZTL* effector (Figures 2B and 4B).
171 The mean FRP was 24.1 ± 0.6 h in the experiment dual-ZTLox#1, which was similar to that without
172 the effector (Table S1). It is noteworthy that *AtCCA1::LUC*+ bioluminescence traces in rhythmic cells
173 (RAE<0.2) in case of dual-ZTLox#1 showed a waveform and phase similar to those of the
174 *CaMV35S::PtRLUC* bioluminescence rhythm (Figures 4A and 4B). This *CaMV35S::PtRLUC*-type
175 bioluminescence rhythm exhibited by *AtCCA1::LUC*+ was also observed in the single reporter
176 experiment with *LmZTL* overexpression (Figure S3). This indicates that the *AtCCA1::LUC*+
177 transfected cells are capable of producing *CaMV35S*-type bioluminescence rhythm when the clock-
178 gene circuit is disrupted by the overexpression of *LmZTL*. Those cells in which the TTFL oscillator is
179 disrupted may therefore have the potential to produce the *CaMV35S::PtRLUC*-type bioluminescence
180 rhythm with any luciferase reporter in the co-transfection experiments.

181 In transgenic *Arabidopsis* overexpressing *LUX* (*PCL*), dampening of the rhythmic expression
182 of clock-genes has been reported.[21] In *L. minor*, *LmLUX* overexpression shortened the FRP of
183 *AtCCA1::LUC*+ rhythm with an amplitude similar to that in the experiment without the effector (Figures
184 4D, 4F and Table S1). By contrast, *LmLUX* overexpression did not affect the *CaMV35S::PtRLUC*
185 rhythm in the analyzed cells. Every cell showed a waveform and FRP similar to those in experiments
186 without the effector (Figures 2D, 4E, 4F and Table S1). Consequently, *LmLUX* overexpression
187 shortened the FRPs of the *AtCCA1::LUC*+ rhythm compared with those of the *CaMV35S::PtRLUC*
188 rhythm in most of the analyzed cells (Figures S2 and S4). This indicated that *LmLUX* overexpression
189 disrupted the clock gene circuit in the transfected cells without affecting the *CaMV35S::PtRLUC*
190 rhythm.

191 Overexpression of *LgELF3* in the cells of *Lemna gibba* resulted in perturbation of light
192 entrainment, and an increase in the number of cells with unstable rhythms and longer FRPs.[16] In *L.*
193 *minor*, overexpression of *LmELF3* caused unstable *AtCCA1::LUC*+ cellular rhythms and longer FRPs
194 in dual-reporter experiments (Figure 4G, 4I and Table S1). By contrast, cellular *CaMV35S::PtRLUC*
195 bioluminescence showed a stable rhythm and no alteration of FRP (Figure 4H, 4I and Table S1). This
196 indicated that overexpression of *LmELF3* modified the clock gene circuit in the transfected cells
197 without affecting the *CaMV35S::PtRLUC* rhythm. In single-reporter experiments, many cells co-
198 transfected with *LmELF3* overexpressing effector showed unstable *AtCCA1::LUC*+ rhythm but stable

199 *CaMV35S::PtRLUC* rhythm (Table S2). These results suggested that *LmELF3* overexpression
200 impaired the clock gene circuit in the transfected cells that maintained the *CaMV35S::PtRLUC* rhythm.
201 Results of the overexpression of the three clock genes, therefore, indicate that the
202 *CaMV35S::PtRLUC* bioluminescence rhythm is generated on a cellular level without direct regulation
203 by the clock gene circuit in the same cell.
204
205 Disruption of the *CaMV35S::PtRLUC* bioluminescence rhythm in a hypertonic medium
206 While the co-transfection of a clock-gene overexpressing effector affects the circadian clock in the
207 luciferase-expressing cells, most cells not transfected by particle bombardment are unlikely to be
208 affected by the effector. Therefore, it raises the possibility that the *CaMV35S::PtRLUC* rhythm in the
209 transfected cells is supported by surrounding tissues with normal circadian rhythms. In order to disrupt
210 the intercellular signal transmission to the transfected cells, we exposed the frond to hypertonic
211 medium to cause plasmolysis. We performed dual-color monitoring experiment on the fronds being
212 subjected to NF medium with 500 mM mannitol (Figure 5). Plasmolysis of cells that were transfected
213 with *CaMV35S::GFP-h* by particle bombardment was confirmed in the frond that was subjected to the
214 hypertonic medium (Figure S5). The *AtCCA1::LUC*+ rhythm was observed in all analyzed cells in
215 hypertonic conditions, although a period lengthening appeared (Figure 5A, 5C and Table S1).
216 Interestingly though, the *CaMV35S::PtRLUC* rhythm disappeared in the same cells (Figure 5B, 5C
217 and Table S1). Similar results were obtained for the circadian rhythmicity of each reporter in the single
218 reporter experiments involving hypertonic treatment (Tables S2). The disappearance of the
219 *CaMV35S::PtRLUC* rhythm in cells showing stable *AtCCA1::LUC*+ rhythm strongly suggests that the
220 *CaMV35S::PtRLUC* rhythm is non-cell-autonomously generated with the support of surrounding
221 tissues.
222
223
224 **Discussion**
225 In this study, we have demonstrated that the *CaMV35S::PtRLUC* bioluminescence rhythm is not
226 governed by the clock gene circuit in the expressing cells but requires the support of surrounding
227 tissues in the plant. The maintenance of high synchrony in the *CaMV35S::PtRLUC* rhythm between
228 cells in the frond stands in contrast to the dyssynchronous nature of the *AtCCA1::LUC*+ rhythm, that
229 is linked to the clock gene circuit (Figure 2F).[17] This indicates distinct characteristics of cell-
230 autonomous and non-cell-autonomous rhythms. Figure 6 shows a conceptual framework of
231 generation of these rhythms in individual cells in the plant. In each cell, TTFL drives the cell-
232 autonomous rhythms such as the *AtCCA1::LUC*+ rhythm. The non-cell-autonomous rhythms such as
233 the *CaMV35S::PtRLUC* rhythm are driven by symplast/apoplast mediation. Circadian rhythms that
234 are driven by changes in concentrations of ions and small molecules and the water flux potentially
235 belong to this category. Circadian-regulated solute transporters of individual cells appear to generate
236 these circadian rhythms,[22] while changes in the concentrations of these diffusive elements inevitably

involve extracellular factors that are shared by the plant cells. These non-cell-autonomous rhythms can be driven at an organismal level. The rhythmicity at the organismal level depends on the integration of temporal information between cellular clocks. Therefore, a certain degree of synchrony between them is required to generate the non-cell-autonomous rhythms. This framework effectively explains the distinct characteristics of the *AtCCA1::LUC+* and *CaMV35S::PtRLUC* rhythms. Diffusive elements such as luciferin, magnesium ions, protons, ATP, and oxygen that influence the luciferase enzyme activity[23] may oscillate in a circadian manner in duckweed. In fact, a circadian rhythm of the absorption of ions such as potassium and magnesium ions, has been reported in the duckweed species *Lemna gibba*.[24,25] It was also reported that *L. gibba* showed circadian rhythms in respiratory metabolism including the pentose phosphate pathway under constant light.[26] The circadian rhythm at an organismal level should show higher synchrony between cells than the cell-autonomous rhythm. Thus, the *CaMV35S::PtRLUC* rhythm can be more synchronous than the *AtCCA1::LUC+* rhythm in a frond. Notably the *CaMV35S::PtRLUC* rhythm is lost or is rendered unstable in a frond with cellular clocks in an asynchronous state.[12]

An important finding of this study is that physiological rhythms in individual cells are not always governed by their own cellular circadian clocks. These rhythms can stay stable in the plant even when the synchrony between the cellular clocks of its cells becomes low. This allows imprecision of individual cellular clocks and uneven circadian properties between cells. Indeed, in a *L. gibba* frond under constant light, each cellular clock showed an unstable FRP (SD for cycle-to-cycle variation: 2.45 h) and a relatively large variation of FRP was reported between cells (SD 1.11 h).[17] The highly synchronous rhythm independent of the quality of individual cellular clocks would effectively work without the need to maintain the accuracy of each clock.

Our results clearly indicate that the *CaMV35S::PtRLUC* rhythm was maintained in the cells in which the *AtCCA1::LUC+* rhythm was disrupted by *ZTL* overexpression. This strongly suggests that the clock gene circuit is dispensable for the *CaMV35S::PtRLUC* rhythm in the cell. This does not necessarily mean that the gene circuit of the plant cells is completely dispensable for the *CaMV35S::PtRLUC* rhythm. The *ZTL* overexpression after transfection using particle bombardment was expected to disrupt the gene circuit only in the transfected cells, and most cells in the plant were not affected. These unaffected cells were probably responsible for the non-cell-autonomous rhythm at an organismal level. The stable transformation method has been established for *L. minor*,[18,27] and transgenic plants overexpressing *ZTL* would be an interesting model for studying the necessity of the clock gene circuit for the *CaMV35S::PtRLUC* rhythm. In a previous study, the circadian rhythms of bioluminescence reporters in roots (rootstocks) of *Arabidopsis* clock mutants were partially restored by grafting wild type shoot apex.[28] In that case, it appears that the cellular circadian clock in the roots was restored. Therefore, the mechanism for generating the rhythm in *Arabidopsis* may differ from that of the *CaMV35S::PtRLUC* rhythm in duckweed. In fact, multiple mechanisms may exist to generate non-cell-autonomous circadian rhythms in plants.

274 Intercellular communication is an interesting aspect of the plant circadian system.[11,29]
275 Synchronization between neighboring cellular clocks and long-distance clock communication have
276 been previously reported.[17,18,28,30–34] A non-cell-autonomous physiological rhythm with a high spatial
277 synchrony can effectively function in the synchronization process between cellular clocks if the clock
278 gene circuit is affected by the physiological rhythm in individual cells. Calcium is a potential mediator
279 of this intercellular communication because cytosolic free calcium in plant cells is a physiological
280 circadian output and is also involved in the regulation of the circadian clock.[35,36] Interestingly, it has
281 been suggested that the calcium rhythm and the *Cab* (*Lhcb*) gene expression rhythm are separately
282 controlled for the determination of their FRPs and the oscillation generation by the clock gene circuit.[5,7]
283 It is therefore worth investigating whether the calcium rhythm is non-cell-autonomous.
284 The mechanisms that generate the *CaMV35S::PtRLUC* bioluminescence rhythm are
285 currently unknown.[12] In the conceptual framework (Figure 6), physiological conditions associated with
286 the bioluminescence reaction in the cells seem to post-transcriptionally mediate the rhythm. Circadian
287 rhythms in the levels of ions and/or metabolites at an organismal level may bring about the
288 bioluminescence rhythm.[22,29,37] These rhythms may not be the simple sum of the individual cellular
289 rhythms in the plant because the FRP of the *CaMV35S::PtRLUC* rhythm is different from that of the
290 *AtCCA1::LUC*+ rhythm (Table S1). Further studies of such non-cell-autonomous rhythms should
291 improve the understanding the circadian systems in plants, which involve various cells with cell-
292 autonomous circadian clocks.
293
294
295 **Materials and Methods**
296 Plant material and growth conditions
297 *Lemna minor* 5512 was maintained in NF medium with 1% sucrose under constant light conditions in
298 a temperature-controlled room (25 ± 1 °C), as previously described.[13] The white light (~20 μE m^{-2} s^{-}
299 ^{1}) was generated by fluorescent lamps (FLR40SEX-W/M/36-HG, NE, Japan). Plants were grown on
300 60 ml of the medium in 200-ml Erlenmeyer flasks plugged with cotton. New stock cultures were made
301 weekly, and well-grown plants were used for the experiments. To entrain the circadian rhythm, plants
302 were cultured under at least three 12 h light/12 h dark cycles in an incubator (MIR-153, Panasonic,
303 Japan) before starting the experiments.
304
305 Luciferase reporters
306 As circadian bioluminescent reporters, we used *pUC-AtCCA1::intron-LUC*+ (*AtCCA1::LUC*+), and
307 *pUC18-CaMV35S::PtRLUC* (*CaMV35S::PtRLUC*), which have been described previously[12]. PtRLUC
308 is a red-shift mutant (S246H/H347A) of Emerald luciferase (ELuc) from Brazilian click beetle
309 (*Pyrearinus termitilluminans*).[38]
310
311 Clock-gene overexpression effectors

312 *pUC18-CaMV35S::LmZTL*, *pUC18-CaMV35S::LmLUX*, and *pUC18-CaMV35S::LmELF3* were
313 constructed as follows. Coding regions of *LmZTL*, *LmLUX*, and *LmELF3* from *Lemna minor* 5512
314 were amplified using PCR with the following primer sets:
315 CgcggccgcCACCATGGAGTGGAATAGTGATTCG and CggcgcgccTTAAATGAGCTCCGAGAAGCC
316 for *LmZTL*, CgcggccgcATGGCGGACGGTGATGGCGG and
317 CggcgcgccTTATTTGTAACCGGGAGAAACATGG for *LmLUX*,
318 CgcggccgcATGAAGAGAGGGAGAGAGGAAGATAAG and
319 CggcgcgccCTACAGCGGATCGTATCCCTG for *LmELF3*. Primer sequences for each gene were
320 designed based on the genome sequence of *Lemna minor* 5500.[39] The small-letter 8-b sequence in
321 each primer sequence represents a restriction enzyme recognition site (*Not*1 for forward primer and
322 *Asc*1 for reverse primer). cDNA that was synthesized from total RNA of *L. minor* 5512 using ReverTra
323 Ace (TOYOBO, Japan) was used as the template for the PCR. The total RNA was extracted from the
324 whole plant using NucleoSpin RNA (Takara, Japan). The amino acid sequences of LmZTL and
325 LmELF3 are identical in the strains 5500 and 5512. Compared with the strain 5500, the amino acid
326 sequence of LmLUX in strain 5512 contains four amino acid substitutions and an insertion of two
327 amino acids. The amplicon of each gene was cloned into *pENTR-D-TOPO* (Invitrogen, MA, USA) with
328 an additional multi-cloning site. Using the LR reaction, the coding region in this plasmid was integrated
329 into *pUC18-CaMV35S-attR1-attR2-NosT*, in which the *att*R1-*att*R2 sequence (Invitrogen) was located
330 between the *CaMV35S* promoter and the Nos terminator.
331
332 Particle bombardment and bioluminescence monitoring
333 Reporter constructs were introduced into *L. minor* plants by particle bombardment as described
334 previously.[13] In both single- and dual-reporter experiments, the amounts of plasmid DNA coding for
335 *AtCCA1::LUC+* and *CaMV35S::PtRLUC*, were 2 μg, and 0.2 μg, respectively. In co-transfection
336 experiments, 1 μg overexpression effector of a clock gene was added to the reporter(s).
337 Dual-color bioluminescence monitoring at a single cell level was carried out as described previously.[12]
338 In short, the imaging system consisted of an EM-CCD camera (ImagEM C9100-13; Hamamatsu
339 Photonics, Japan) with a lens (VS-50085/C 0.85/50mm; VS Technology, Japan), a handmade filter
340 changer with a rotation motor (ARS-4036-GM; Chuo Precision Industrial Co., Japan), a handmade
341 motor-driven stage with rotation and z-axis stages (ARS-6036-GM and ALV-902-HP; Chuo Precision
342 Industrial Co., Japan), and an illuminating system with an end-emitting fiber optics guiding LED white
343 light (approximately 30 μE m^{-2} s^{-1}; RFB2-20SW; CCS Inc, Japan). These devises were set in a
344 lightproof box in an incubator (25 ± 1°C). A green-pass filter (PB0530/080; ⌀49.7 mm; Asahi Spectra,
345 Japan) and red-pass filter (PB0630/040; ⌀49.7 mm; Asahi Spectra) were placed in slots in the filter
346 changer, and one slot was left empty to capture unfiltered images. By controlling this imaging system
347 using PC software (HOKAWO; Hamamatsu Photonics), a series of bioluminescence images for a
348 sample dish were automatically captured every 1 h. Based on the intensities of the filtered
349 bioluminescence of a luminous cell expressing both the reporters, the bioluminescence intensity of

350 each reporter at every time point was calculated. The same imaging protocol was used for single-
351 reporter experiments.
352 Bioluminescence monitoring in the hypertonic conditions (NF medium with 1% sucrose and 500 mM
353 mannitol) was carried out using a plant that was transferred from the normal medium conditions just
354 before the start of the monitoring.
355
356 Fluorescence imaging
357 A fluorescent reporter (*CaMV35S::GFP-h*)[40] was transfected into the duckweed plants, and GFP
358 fluorescence-positive cells were observed under a confocal microscope (LSM510-META; Carl Zeiss,
359 https://www.zeiss.com) as described previously.[41]
360
361 Time series analysis
362 The criteria for luminous spots that were used for time series analysis were the same as those
363 previously described, except for a change in the lower limit of the ratio of luminescence intensities of
364 a 24 h moving average between *AtCCA1::LUC+* and *CaMV35S::PtRLUC* (from 1/20 to 1/100).[12] The
365 FRPs and RAEs of the bioluminescence traces were estimated using the fast Fourier transform non-
366 linear least squares method, as described previously.[12] The peak times of bioluminescence traces
367 were estimated by local quadratic curve fitting, as described previously.[12]
368 Phase $\theta(t)$ of the bioluminescence rhythms $x(t)$ was defined as follows

369 $$\theta(t) = 2\pi \frac{t - t_p^k}{t_p^{k+1} - t_p^k} \ (t^k \leq t < t^{k+1}, k = 1 \ldots M)$$

370 where t_p^k represents the occurrence time of the kth peak of $x(t)$ and M represents the total
371 number of peaks. Data analysis codes are available at https://github.com/ukikusa/circadian_analysis
372
373 Synchronization index
374 To assess the synchrony between cellular rhythms within a plant, the SI, which is known as the order
375 parameter in the Kuramoto model, was calculated at each time point as follows

376 $$R(t) = \frac{1}{N} \left| \sum_k exp(i\theta_k(t)) \right|$$

377 where $\theta_k(t)$ is the phase of the kth cell at time t, and N is the number of cells.
378 The SI at a given time was calculated if the ratio of cells of which the phase was defined was more
379 than 80% of rhythmic cells. For dual reporter experiments, cells showing both rhythms were analyzed.
380
381
382 **References**
383 1. Sweeney, B.M. (1987). Rhythmic phenomena in plants 2nd ed. (Academic Press).
384 2. Nohales, M.A., and Kay, S.A. (2016). Molecular mechanisms at the core of the plant
385 circadian oscillator. Nat. Struct. Mol. Biol. *23*, 1061–1069.

386 3. Sanchez, S.E., Rugnone, M.L., and Kay, S.A. (2020). Light perception: a matter of time.
387 Mol. Plant *13*, 363–385.
388 4. Somers, D.E., Webb, A.A.R., Pearson, M., and Kay, S.A. (1998). The short-period mutant,
389 toc1-1, alters circadian clock regulation of multiple outputs throughout development in *Arabidopsis*
390 *thaliana*. Development, 485–494.
391 5. Xu, X., Hotta, C.T., Dodd, A.N., Love, J., Sharrock, R., Lee, Y.W., Xie, Q., Johnson, C.H.,
392 and Webb, A.A.R. (2007). Distinct light and clock modulation of cytosolic free Ca^{2+} oscillations and
393 rhythmic *CHLOROPHYLL A/B BINDING PROTEIN2* promoter activity in *Arabidopsis*. Plant Cell *19*,
394 3474–3490.
395 6. Nohales, M.A. (2021). Spatial organization and coordination of the plant circadian system.
396 Genes *12*, 442.
397 7. Sai, J., and Johnson, C.H. (1999). Different circadian oscillators control Ca^{2+} fluxes and
398 *lhcb* gene expression. Proc. Natl. Acad. Sci. U.S.A. *96*, 11659–11663.
399 8. Thain, S.C., Murtas, G., Lynn, J.R., McGrath, R.B., and Millar, A.J. (2002). The circadian
400 clock that controls gene expression in Arabidopsis is tissue specific. Plant Physiol. *130*, 102–110.
401 9. Hall, A., Kozma-Bognár, L., Bastow, R.M., Nagy, F., and Millar, A.J. (2002). Distinct
402 regulation of *CAB* and *PHYB* gene expression by similar circadian clocks. Plant J. *32*, 529–537.
403 10. Michael, T.P., Salomé, P.A., and McClung, C.R. (2003). Two *Arabidopsis* circadian
404 oscillators can be distinguished by differential temperature sensitivity. Proc. Natl. Acad. Sci. U.S.A.
405 *100*, 6878–6883.
406 11. McClung, C.R. (2019). The plant circadian oscillator. Biology *8*, 14.
407 12. Watanabe, E., Isoda, M., Muranaka, T., Ito, S., and Oyama, T. (2021). Detection of
408 uncoupled circadian rhythms in individual cells of *Lemna minor* using a dual-color bioluminescence
409 monitoring system. Plant Cell Physiol. *62*, 815–826.
410 13. Muranaka, T., Okada, M., Yomo, J., Kubota, S., and Oyama, T. (2015). Characterisation of
411 circadian rhythms of various duckweeds. Plant Biol. *17*, 66–74.
412 14. Miwa, K., Serikawa, M., Suzuki, S., Kondo, T., and Oyama, T. (2006). Conserved
413 expression profiles of circadian clock-related genes in two *Lemna* species showing long-day and
414 short-day photoperiodic flowering responses. Plant Cell Physiol. *47*, 601–612.
415 15. Serikawa, M., Miwa, K., Kondo, T., and Oyama, T. (2008). Functional conservation of
416 clock-related genes in flowering plants: overexpression and RNA interference analyses of the
417 circadian rhythm in the monocotyledon *Lemna gibba*. Plant Physiol. *146*, 1952–1963.
418 16. Okada, M., Muranaka, T., Ito, S., and Oyama, T. (2017). Synchrony of plant cellular
419 circadian clocks with heterogeneous properties under light/dark cycles. Sci. Rep. *7*, 317.
420 17. Muranaka, T., and Oyama, T. (2016). Heterogeneity of cellular circadian clocks in intact
421 plants and its correction under light-dark cycles. Sci. Adv. *2*, e1600500.
422 18. Ueno, K., Ito, S., and Oyama, T. (2022). An endogenous basis for synchronization manners
423 of the circadian rhythm in proliferating *Lemna minor* plants. New Phytol. *233*, 2203–2215.

19. Plautz, J.D., Straume, M., Stanewsky, R., Jamison, C.F., Brandes, C., Dowse, H.B., Hall, J.C., and Kay, S.A. (1997). Quantitative analysis of *Drosophila period* gene transcription in living animals. J. Biol. Rhythms *12*, 204–217.

20. Somers, D.E., Kim, W.-Y., and Geng, R. (2004). The F-box protein ZEITLUPE confers dosage-dependent control on the circadian clock, photomorphogenesis, and flowering time. Plant Cell *16*, 769–782.

21. Onai, K., and Ishiura, M. (2005). *PHYTOCLOCK 1* encoding a novel GARP protein essential for the *Arabidopsis* circadian clock. Genes to Cells *10*, 963–972.

22. Haydon, M.J., Bell, L.J., and Webb, A.A.R. (2011). Interactions between plant circadian clocks and solute transport. J. Exp. Bot. *62*, 2333–2348.

23. Van Leeuwen, W., Hagendoorn, M.J.M., Ruttink, T., Van Poecke, R., Van Der Plas, L.H.W., and Van Der Krol, A.R. (2000). The use of the luciferase reporter system forin planta gene expression studies. Plant Mol. Biol. Rep. *18*, 143–144.

24. Kondo, T., and Tsudzuki, T. (1978). Rhythm in potassium uptake by a duckweed, *Lemna gibba* G3. Plant Cell Physiol. *19*, 1465–1473.

25. Kondo, T. (1983). Phase shifts of potassium uptake rhythm in *Lemna gibba* G3 due to light, dark or temperature pulses. Plant Cell Physiol. *24*, 659–665.

26. Miyata, H., and Yamamoto, Y. (1969). Rhythms in respiratory metabolism of *Lemna gibba* G3 under continuous illumination. Plant Cell Physiol. *10*, 875–889.

27. Chhabra, G., Chaudhary, D., Sainger, M., and Jaiwal, P.K. (2011). Genetic transformation of Indian isolate of *Lemna minor* mediated by *Agrobacterium tumefaciens* and recovery of transgenic plants. Physiol. Mol. Biol. Plants *17*, 129–136.

28. Takahashi, N., Hirata, Y., Aihara, K., and Mas, P. (2015). A hierarchical multi-oscillator network orchestrates the *Arabidopsis* circadian system. Cell *163*, 148–159.

29. Sorkin, M.L., and Nusinow, D.A. (2021). Time will tell: intercellular communication in the plant clock. Trends Plant Sci. *26*, 706–719.

30. Fukuda, H., Nakamichi, N., Hisatsune, M., Murase, H., and Mizuno, T. (2007). Synchronization of plant circadian oscillators with a phase delay effect of the vein network. Phys. Rev. Lett. *99*, 098102.

31. Fukuda, H., Ukai, K., and Oyama, T. (2012). Self-arrangement of cellular circadian rhythms through phase-resetting in plant roots. Phys. Rev. E *86*, 041917.

32. Wenden, B., Toner, D.L.K., Hodge, S.K., Grima, R., and Millar, A.J. (2012). Spontaneous spatiotemporal waves of gene expression from biological clocks in the leaf. Proc. Natl. Acad. Sci. U.S.A. *109*, 6757–6762.

33. Endo, M., Shimizu, H., Nohales, M.A., Araki, T., and Kay, S.A. (2014). Tissue-specific clocks in *Arabidopsis* show asymmetric coupling. Nature *515*, 419–422.

34. Gould, P.D., Domijan, M., Greenwood, M., Tokuda, I.T., Rees, H., Kozma-Bognar, L., Hall, A.J., and Locke, J.C. (2018). Coordination of robust single cell rhythms in the *Arabidopsis* circadian clock via spatial waves of gene expression. eLife *7*, e31700.

35. Johnson, C.H., Knight, M.R., Kondo, T., Masson, P., Sedbrook, J., Haley, A., and Trewavas, A. (1995). Circadian oscillations of cytosolic and chloroplastic free calcium in plants. Science *269*, 1863–1865.

36. Martí Ruiz, M.C., Hubbard, K.E., Gardner, M.J., Jung, H.J., Aubry, S., Hotta, C.T., Mohd-Noh, N.I., Robertson, F.C., Hearn, T.J., Tsai, Y.-C., et al. (2018). Circadian oscillations of cytosolic free calcium regulate the Arabidopsis circadian clock. Nat. Plants *4*, 690–698.

37. Haydon, M.J., Mielczarek, O., Robertson, F.C., Hubbard, K.E., and Webb, A.A.R. (2013). Photosynthetic entrainment of the *Arabidopsis thaliana* circadian clock. Nature *502*, 689–692.

38. Nishiguchi, T., Yamada, T., Nasu, Y., Ito, M., Yoshimura, H., and Ozawa, T. (2015). Development of red-shifted mutants derived from luciferase of Brazilian click beetle *Pyrearinus termitilluminans*. J. Biomed. Opt. *20*, 101205.

39. Van Hoeck, A., Horemans, N., Monsieurs, P., Cao, H.X., Vandenhove, H., and Blust, R. (2015). The first draft genome of the aquatic model plant *Lemna minor* opens the route for future stress physiology research and biotechnological applications. Biotechnol. Biofuels *8*, 188.

40. Nakano, R.T., Matsushima, R., Ueda, H., Tamura, K., Shimada, T., Li, L., Hayashi, Y., Kondo, M., Nishimura, M., and Hara-Nishimura, I. (2009). GNOM-LIKE1/ERMO1 and SEC24a/ERMO2 are required for maintenance of endoplasmic reticulum morphology in *Arabidopsis thaliana*. Plant Cell *21*, 3672–3685.

41. Muranaka, T., Kubota, S., and Oyama, T. (2013). A single-cell bioluminescence imaging system for monitoring cellular gene expression in a plant body. Plant Cell Physiol. *54*, 2085–2093.

Acknowledgements

We thank Dr. Hiroshi Kori for fruitful discussions and useful advice. This research was supported by the Japan Society for the Promotion of Science KAKENHI [grant numbers JP21J23250 (E.W.), JP19J23441(S.N.), JP16H06864 (T.M.), JP20K06342 (S.I.), JP17KT0022 (T.O.) and JP19H03245(T.O.)], Japan Science and Technology Agency (JST), JST ALCA (JPMJAL1108, T.O.), and JST SATREPS (JPMJSA2004, T.M., S.I., T.O.).

Author contributions

E.W., T.M. and T.O. designed the study. E.W. and T.O. wrote the manuscript. E.W. performed the bioluminescence monitoring experiments and data analysis. S.N. performed plasmolysis. S.I. and M.I. performed molecular cloning. All authors have contributed to the text.

Declaration of interests

The authors declare no competing interests.

Figure 1

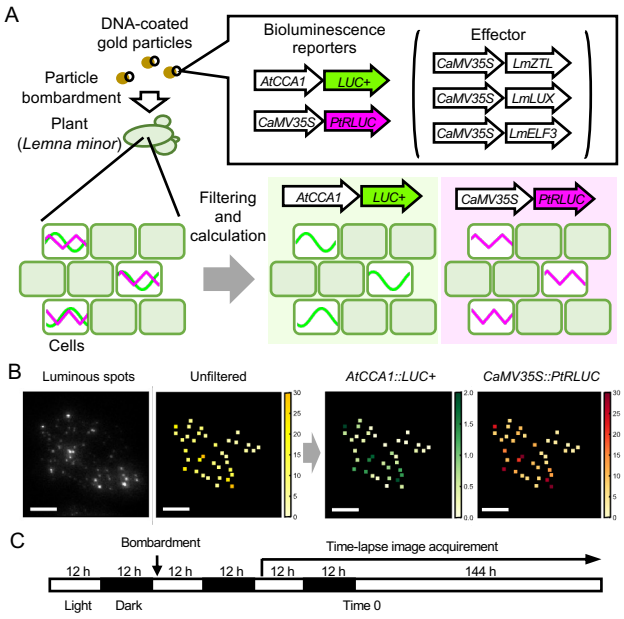

Figure 1. Outline of the dual-color bioluminescence monitoring experiments
(A) Schematic drawing of the measurement of *AtCCA1::LUC+* and *CaMV35S::PtRLUC* bioluminescence at a single-cell level. Bioluminescence reporters were introduced into *Lemna minor* cells by particle bombardment. Filtered cellular bioluminescence was imaged and used for the calculation of luminescence intensities of each reporter. For overexpression experiments, an effector (*CaMV35S::LmZTL*, *CaMV35S::LmLUX* or *CaMV35S::LmELF3*) was co-transfected with the reporters. (B) An example of the reconstruction of cellular luminescence intensities [1000 photons/s] of each reporter. Luminescence intensities of individual cells are color coded. Scale bars are 1 mm. (C) Time schedule of the monitoring experiments. *L. minor* plants that had been cultured under 12 h light 12 h dark cycles were transfected by particle bombardment. The transfected plants were further cultured under 12 h light 12 h dark cycles, and then transferred to the imaging system. Open and closed boxes represent light and dark conditions, respectively. Time 0 is defined as the start of constant light during the time-lapse imaging.

Figure 2

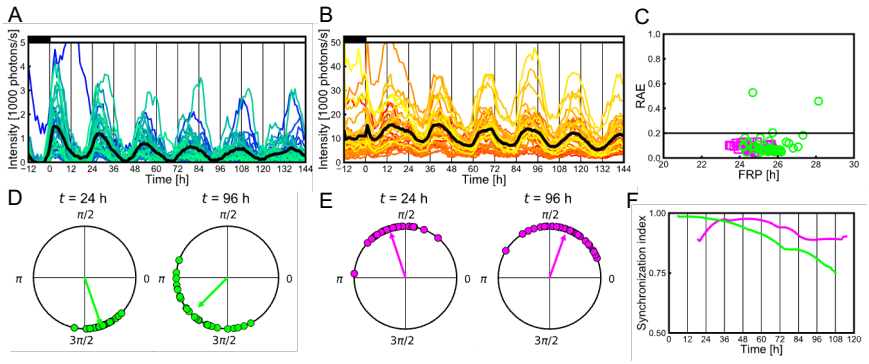

Figure 2. Cellular circadian properties of *AtCCA1::LUC+* and *CaMV35S::PtRLUC* rhythms in the dual-reporter experiment

A total of 37 cells in a frond were analyzed. (A and B) Cellular *AtCCA1::LUC+* (A) and *CaMV35S::PtRLUC* (B) bioluminescence rhythms. The black line represents mean luminescence intensities. Close and open boxes represent light and dark conditions, respectively. (C) The free-running periods (FRPs) and the relative amplitude errors (RAEs) of individual cellular rhythms. Green circles and magenta squares represent *AtCCA1::LUC+* and *CaMV35S::PtRLUC*, rhythms, respectively. Cellular bioluminescence traces with RAE < 0.2 are defined as rhythmic. (D and E) Plots of the phases of *AtCCA1::LUC+* rhythm (D) and *CaMV35S::PtRLUC* rhythm (E) on the unit circle at 24 h and 96 h, respectively. The peak right before 24 h or 96 h is referred to as phase 0 [rad]. The vector represents the vector mean of each plot on the unit circle. The vector length and the angle represent the synchronization index (SI) and a representative phase, respectively, at each time. (F) Temporal changes in the SIs of *AtCCA1::LUC+* (green) and *CaMV35S::PtRLUC* (magenta) rhythms.

Figure 3

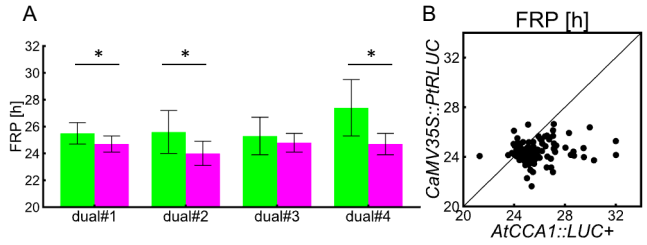

Figure 3 Difference in the free running periods (FRPs) between *AtCCA1::LUC+* and *CaMV35S::PtRLUC* bioluminescence rhythms

Cellular rhythms detected in the four experiments (dual#1: 33 cells, dual#2: 50 cells, dual#3: 18 cells, dual#4: 15 cells) were analyzed. (A) FRPs of *AtCCA1::LUC+* or *CaMV35S::PtRLUC* rhythms in each experiment. Data are expressed as mean ± SD. Asterisk denotes statistically significant difference (Welch's *t* test, $p < 0.01$). (B) A scatterplot of the FRPs between *AtCCA1::LUC+* and *CaMV35S::PtRLUC* rhythms. FRPs of the 116 cells showing the circadian rhythms of both reporters in the four experiments are plotted. The dashed line represents where the FRPs are identical in both rhythms.

Figure 4

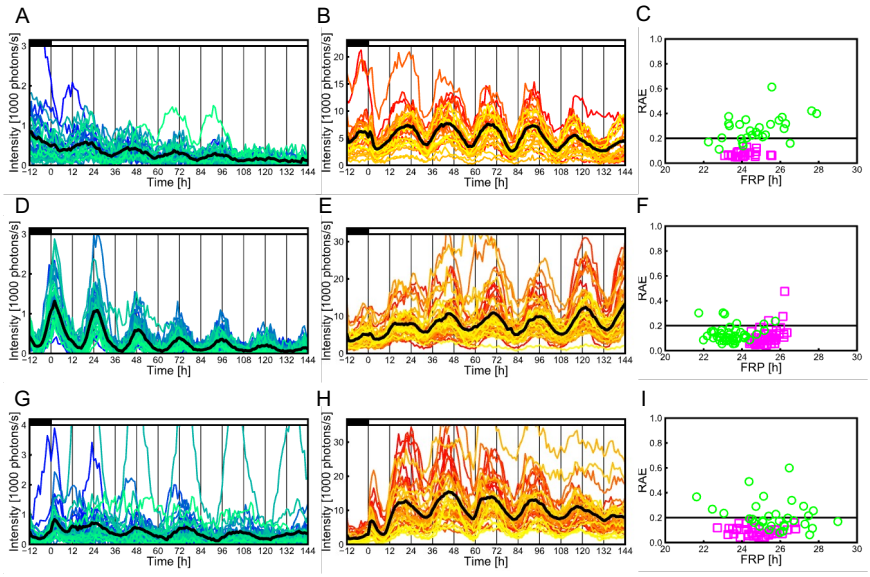

Figure 4. Cellular circadian properties of *AtCCA1::LUC+* and *CaMV35S::PtRLUC* bioluminescence traces in clock-gene overexpression experiments
CaMV35S::LmZTL (dual-ZTLox#1, 29 cells) (A, B, C), *CaMV35S::LmLUX* (dual-LUXox#1, 48 cells) (D, E, F) and *CaMV35S::LmELF3* (dual-ELF3ox#1, 38 cells) (G, H, I) were co-transfected with the dual-color reporters. Cellular *AtCCA1::LUC+* (A, D, G) and *CaMV35S::PtRLUC* (B, E, H) bioluminescence traces are lined in color and a black line in each panel represents mean luminescence intensities. Close and open boxes represent light and dark conditions, respectively. (C, F, I) The free-running periods (FRPs) and the relative amplitude errors (RAEs) of individual cellular rhythms. Green circles and magenta squares represent *AtCCA1::LUC+* and *CaMV35S::PtRLUC* bioluminescence traces, respectively. Cellular bioluminescence traces with RAE < 0.2 are defined as rhythmic.

Figure 5

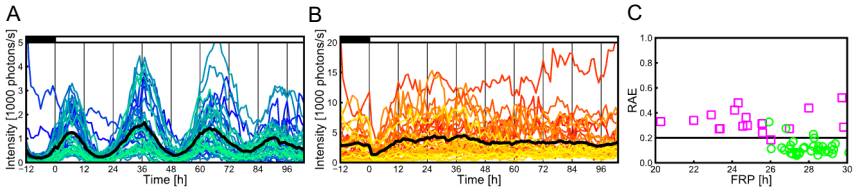

Figure 5. Cellular circadian properties of *AtCCA1::LUC+* and *CaMV35S::PtRLUC* bioluminescence traces in a plant in hypertonic medium

A total of 30 cells in a frond on a hypertonic medium were analyzed for the dual-color reporters. (A and B) Cellular *AtCCA1::LUC+* (A) and *CaMV35S::PtRLUC* (B) bioluminescence traces. A black line represents mean luminescence intensities. Close and open boxes represent light and dark conditions, respectively. (C) Free running periods (FRPs) and the relative amplitude errors (RAEs) of individual cellular rhythms. Green circles and magenta squares represent *AtCCA1::LUC+* and *CaMV35S::PtRLUC* bioluminescence traces, respectively. Cellular bioluminescence traces with RAE < 0.2 are defined as rhythmic.

Figure 6

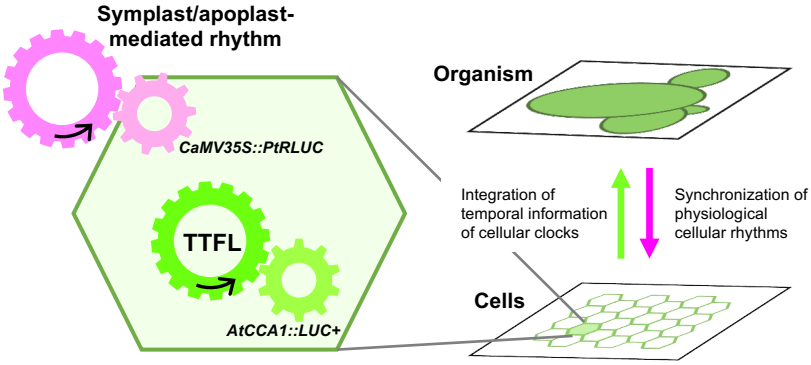

Figure 6. Conceptual framework of the generation of *AtCCA1::LUC+* and *CaMV35S::PtRLUC* bioluminescence rhythms

The *AtCCA1::LUC+* bioluminescence rhythm is generated by the TTFLs in individual cells. The *CaMV35S::PtRLUC* bioluminescence rhythm is a symplast/apoplast-mediated rhythm. Temporal information of cellular clocks is integrated to generate physiological symplast/apoplast-mediated rhythms at an organismal level. These physiological rhythms are synchronous between cells.

Figure S1

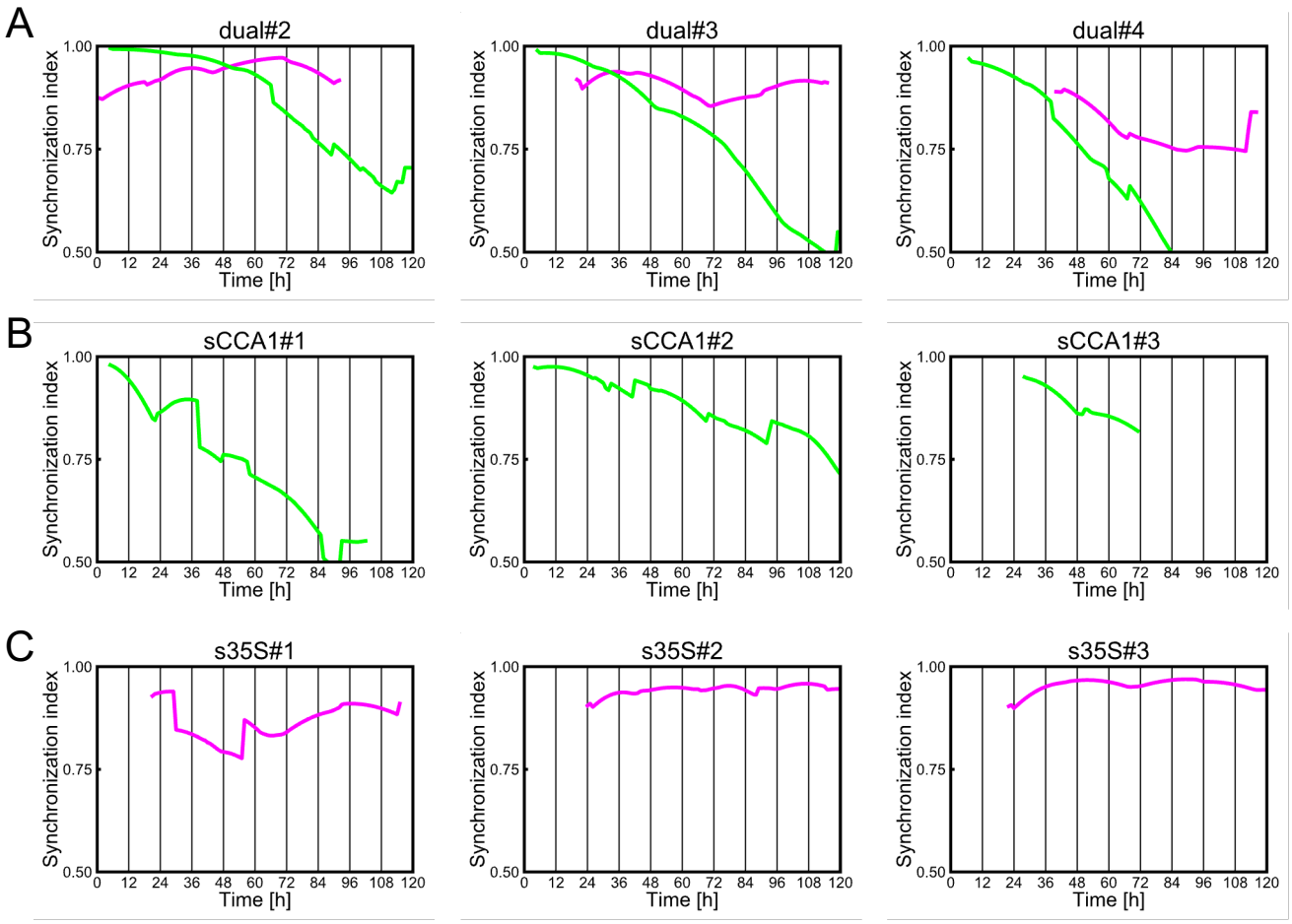

Figure S1. Temporal changes in the synchronization index (SI) of *AtCCA1::LUC+* (green) and *CaMV35S::PtRLUC* (magenta) rhythms in dual and single reporter experiments
(A) Dual-reporter experiments (dual#2-#4), (B) Single-reporter experiments for the *AtCCA1::LUC+* rhythm (sCCA1#1-#3), (C) Single-reporter experiments for the *CaMV35S::PtRLUC* rhythm (s35S#1-#3).

Figure S2

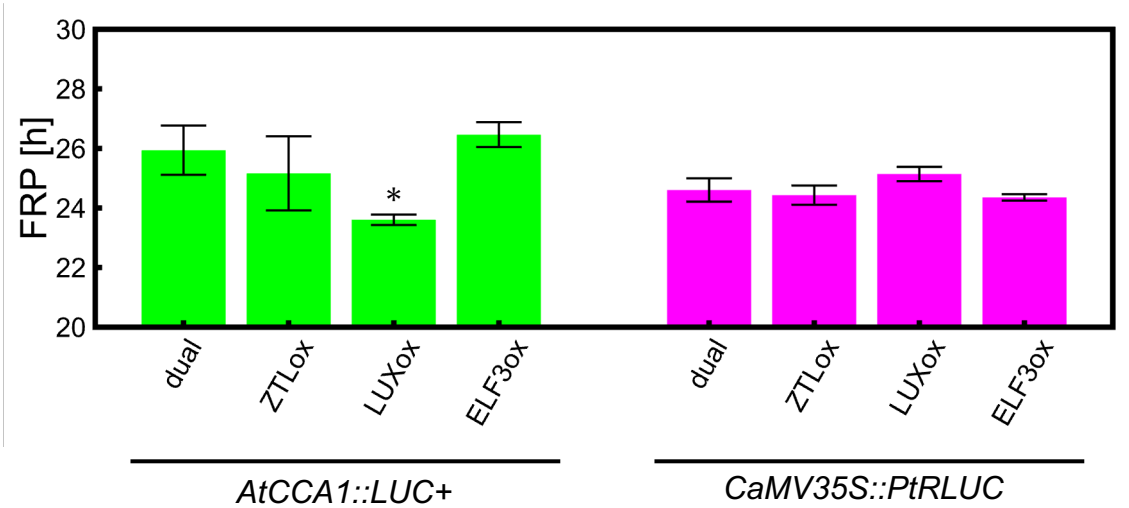

Figure S2. Free running periods (FRPs) of *AtCCA1::LUC+* and *CaMV35S::PtRLUC* bioluminescence rhythms in overexpression experiments
FRPs of cellular bioluminescence rhythms in the control (dual; dual#1-#4), *LmZTL* (ZTLox; dual-ZTLox#1-#3), *LmLUX* (LUXox; dual-LUXox#1-#3) and *LmELF3* (ELF3ox; dual-ELF3ox#1-#3) overexpression experiments. Data are expressed as mean ± SE. Asterisk denotes statistically significant difference (Welch's *t* test, $p < 0.05$).

Figure S3

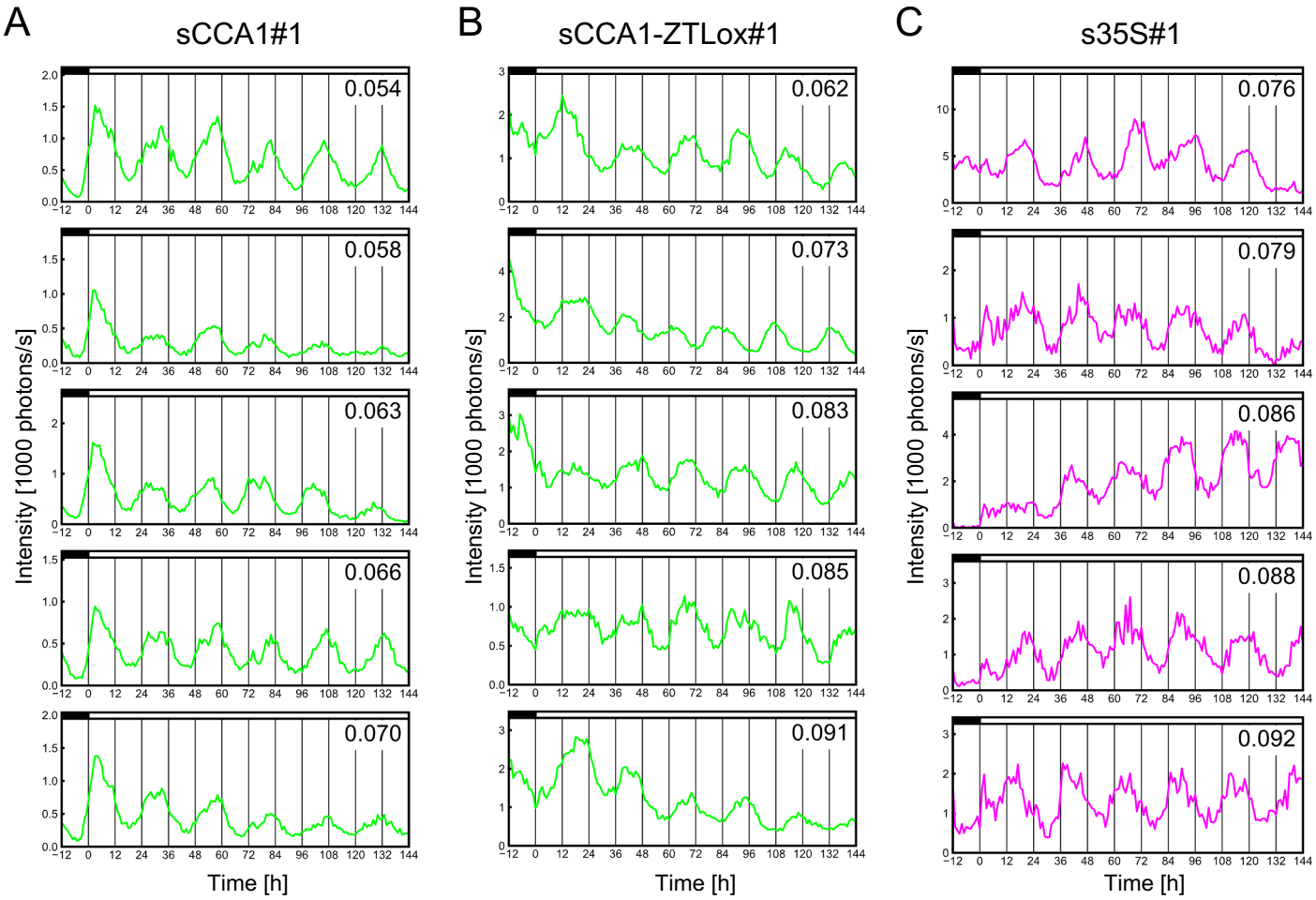

Figure S3. Cellular *AtCCA1::LUC*+ bioluminescence rhythms in an *LmZTL* overexpression experiment with single-reporter

Examples of bioluminescence rhythms of individual cells in single-reporter experiments: sCCA1#1 (A), sCCA1-ZTLox#1 (B), and s35S#1 (C). The cellular bioluminescence rhythms with the five lowest relative amplitude error (RAE) values in each experiment are shown in ascending order. The RAE is indicated in each graph. Close and open boxes represent light and dark conditions, respectively.

Figure S4

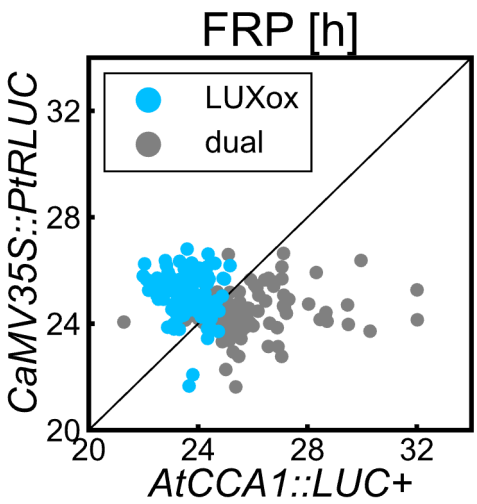

Figure S4. A scatterplot of the free-running periods (FRPs) between *AtCCA1::LUC+* and *CaMV35S::PtRLUC* rhythms in dual-reporter experiments with or without *CaMV35S::LmLUX*
FRPs of the 132 cells showing the circadian rhythms of both reporters in the three overexpression experiments (dual-LUXox#1-#3) are plotted with blue dots. FRPs of the 116 cells showing the circadian rhythms of both reporters in the four experiments without the effector (dual#1-#4) are plotted with gray dots (the same plots as those in Figure 3B). The dashed line represents where the FRPs are identical in both rhythms.

Figure S5

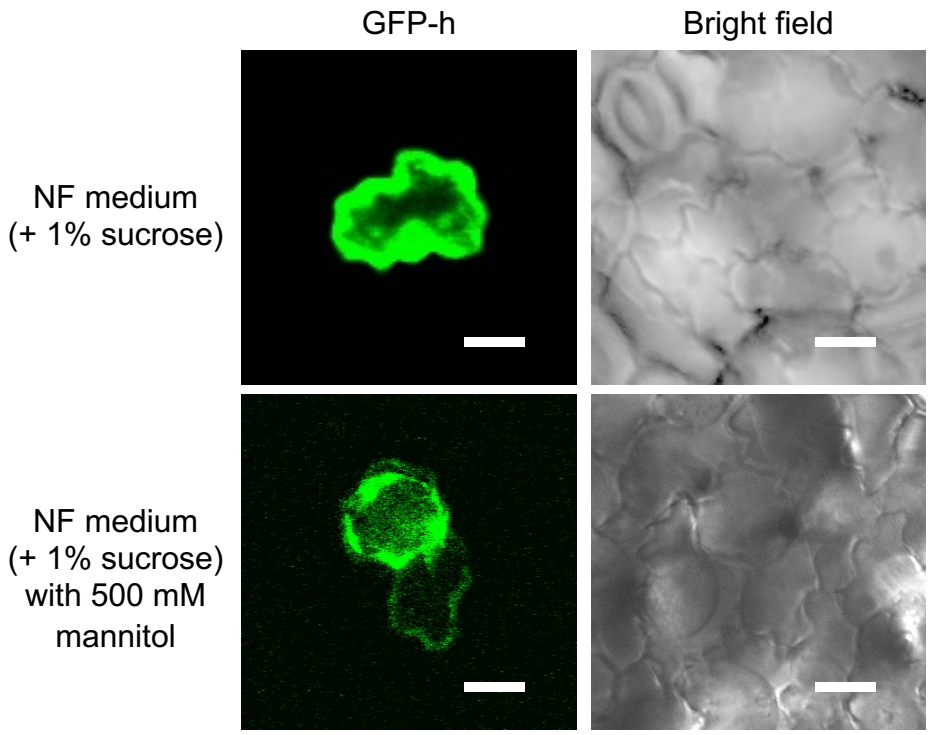

Figure S5. Plasmolysis of cells under hypertonic conditions
GFP fluorescence images of cells that were transfected with an endoplasmic reticulum (ER) localized GFP reporter (*CaMV35S::GFP-h*) and bright field images are shown. An epidermal cell of an *L. minor* plant in NF medium with 1% sucrose and that in NF medium with 1% sucrose and 500 mM mannitol are shown. Bars represent 10 μm.

Table S1. Summary of the quantitative analysis of cellular bioluminescence rhythms in dual reporter experiments

Experiment name	# Identified cells	# Analyzed cells	# Rhythmic in both reporters	*AtCCA1::LUC+*					*CaMV35S::PtRLUC*				
				# Rhythmic cells	Rhythmic ratio	FRP[1] [h]	Phase [rad]	SI	# Rhythmic cells	Rhythmic ratio	FRP[1] [h]	Phase [rad]	SI
dual#1	52	37	33	33	0.89	25.5 ± 0.8 (25.5 ± 0.8)	5.045	0.979	37	1	24.7 ± 0.6 (24.7 ± 0.6)	1.89	0.921
dual#2	61	54	50	50	0.93	25.6 ± 1.6 (25.6 ± 1.6)	4.977	0.986	54	1	24.0 ± 0.7 (24.0 ± 0.7)	0.334	0.919
dual#3	41	20	18	18	0.9	25.3 ± 1.4 (25.3 ± 1.4)	5.204	0.958	20	1	24.8 ± 0.7 (24.8 ± 0.8)	1.463	0.909
dual#4	35	17	15	15	0.88	27.4 ± 2.1 (27.4 ± 2.1)	4.307	0.926	17	1	25.0 ± 0.9 (25.0 ± 0.9)	1.495	0.878
dual-ZTLox#1	41	29	6	6	0.21	23.9 ± 1.3 (23.9 ± 1.3)	1.081	0.807	29	1	24.1 ± 0.6 (24.1 ± 0.4)	0.701	0.981
dual-ZTLox#2	24	10	3	3	0.3	26.9 ± 3.2 (26.9 ± 3.2)	2.678†	0.946†	10	1	24.4 ± 2.2 (24.5 ± 0.8)	1.767†	1†
dual-ZTLox#3	33	8	4	4	0.5	24.7 ± 1.0 (24.7 ± 1.0)	1.899	0.839	8	1	24.7 ± 0.3 (24.8 ± 0.4)	1.978	0.991
dual-LUXox#1	78	48	39	41	0.85	23.3 ± 0.7 (23.4 ± 0.7)	5.897	0.981	44	0.92	25.3 ± 0.5 (25.2 ± 0.5)	0.974	0.936
dual-LUXox#2	60	54	37	41	0.76	23.7 ± 0.7 (23.7 ± 0.6)	6.045	0.976	46	0.85	25.3 ± 0.9 (25.4 ± 0.9)	1.325	0.932
dual-LUXox#3	66	64	56	58	0.91	23.8 ± 0.6 (23.7 ± 0.6)	5.905	0.983	60	0.94	24.8 ± 0.7 (24.8 ± 0.7)	0.971	0.896
dual-ELF3ox#1	52	38	20	21	0.55	26.5 ± 1.7 (26.6 ± 1.7)	5.891	0.505	37	0.97	24.5 ± 2.2 (24.4 ± 2.9)	0.966	0.901
dual-ELF3ox#2	59	55	10	14	0.25	26.0 ± 1.4 (25.9 ± 1.2)	5.282	0.637	51	0.93	24.1 ± 1.1 (24.2 ± 1.4)	1.199	0.841
dual-ELF3ox#3	32	20	3	7	0.35	27.3 ± 1.6 (26.9 ± 1.3)	3.136	0.901	13	0.65	23.8 ± 0.8 (24.5 ± 0.4)	1.471†	0.957†
dual-hyper#1	37	36	0	33	0.92	28.2 ± 1.2 (N.A)	N.A	N.A	1	0.03	26.0 (N.A)	N.A	N.A
dual-hyper#2	32	13	0	6	0.46	28.1 ± 1.3 (N.A)	N.A	N.A	0	0	N.A (N.A)	N.A	N.A
dual-hyper#3	47	46	2	45	0.98	27.9 ± 1.1 (30.7 ± 2.0)	4.29†	1†	2	0.04	23.4 ± 0.4 (23.4 ± 0.4)	5.734†	1†
dual-hyper#4	26	18	0	15	0.83	27.9 ± 1.7 (N.A)	N.A	N.A	0	0	N.A (N.A)	N.A	N.A

[1]Mean FRP ± SD for the cells showing the circadian rhythm of the reporter (top), and for those showing the circadian rhythms of both reporters (bottom and in parentheses).
†The hypothesis that specifies a unique spread of directions in the unit circle is not rejected (Rayleigh test, $p > 0.01$).
N.A: Not applicable.

Table S2. Summary of the quantitative analysis of cellular bioluminescence rhythms in single reporter experiments

			AtCCA1::LUC+					*CaMV35S::PtRLUC*				
Experiment name	# Identified cells	# Analyzed cells	# Rhythmic cells	Rhythmic ratio	FRP[1] [h]	Phase [rad]	SI	# Rhythmic cells	Rhythmic ratio	FRP[1] [h]	Phase [rad]	SI
sCCA1#1	21	21	19	0.9	25.4 ± 1.3	5.558	0.865	-	-	-	-	-
sCCA1#2	43	42	42	1	24.6 ± 0.8	5.654	0.954	-	-	-	-	-
sCCA1#3	18	15	10	0.67	25.1 ± 1.0	5.284	0.983	-	-	-	-	-
s35S#1	29	22	-	-	-	-	-	19	0.86	23.4 ± 2.7	1.087	0.937
s35S#2	47	47	-	-	-	-	-	45	0.96	24.6 ± 0.5	0.706	0.905
s35S#3	53	52	-	-	-	-	-	50	0.96	24.7 ± 0.6	0.819	0.899
sCCA1-ZTLox#1	35	35	17	0.49	23.7 ± 2.4	1.847	0.819	-	-	-	-	-
sCCA1-ZTLox#2	33	33	22	0.67	24.5 ± 0.6	1.774	0.906	-	-	-	-	-
s35S-ZTLox#1	37	37	-	-	-	-	-	35	0.95	24.1 ± 0.7	0.384	0.886
s35S-ZTLox#2	38	38	-	-	-	-	-	36	0.95	24.7 ± 0.9	0.297	0.953
sCCA1-LUXox#1	34	32	31	0.97	23.6 ± 0.8	5.975	0.932	-	-	-	-	-
sCCA1-LUXox#2	26	23	21	0.91	23.6 ± 1.2	5.713	0.972	-	-	-	-	-
s35S-LUXox#1	51	51	-	-	-	-	-	51	1	24.6 ± 0.5	1.118	0.923
s35S-LUXox#2	44	44	-	-	-	-	-	41	0.93	25.0 ± 0.9	1.342	0.905
sCCA1-ELF3ox#1	37	37	25	0.68	27.0 ± 3.4	5.147	0.53	-	-	-	-	-
s35S-ELF3ox#1	57	56	-	-	-	-	-	55	0.98	22.8 ± 1.0	0.881	0.856
s35S-ELF3ox#2	68	68	-	-	-	-	-	53	0.78	22.3 ± 1.4	1.269	0.872

[1]Mean FRP ± SD for rhythmic cells.